Glycobiology, 2015, vol. 25, no. 2, 225–240
doi: 10.1093/glycob/cwu105
Advance Access Publication Date: 1 October 2014
Original Article

OXFORD

Original Article

Golgi *N*-glycan branching *N*-acetylglucosaminyltransferases I, V and VI promote nutrient uptake and metabolism

Anas M Abdel Rahman[2,3,†], Michael Ryczko[3,4,†], Miyako Nakano[6,7,†], Judy Pawling[3], Tania Rodrigues[3,4], Anita Johswich[3], Naoyuki Taniguchi[6], and James W Dennis[1,3,4,5]

[3]Lunenfeld-Tanenbaum Research Institute, Mount Sinai Hospital, 600 University Avenue, Room #988, Toronto, ON, Canada M5G1X5, [4]Department of Molecular Genetics, [5]Department of Laboratory Medicine and Pathobiology, University of Toronto, Toronto, ON, Canada M5G1X5, [6]Disease Glycomics Team, Systems Glycobiology Research Group, Chemical Biology Department, RIKEN-Max Planck Joint Research Center, RIKEN Global Research Cluster, Wako, Saitama 351-0198, Japan, and [7]Graduate School of Advanced Sciences of Matter, Hiroshima University, Hiroshima 739-8530, Japan

[1]To whom correspondence should be addressed: Tel: +1-416-586-8233; Fax: +1-416-586-8857; e-mail: dennis@lunenfeld.ca

[2]Present address: Department of Genetics, Research Center, King Faisal Specialist Hospital and Research Center (KFSHRC), Riyadh 11211, Kingdom of Saudi Arabia.
[†]Co-first authors.

Received 30 July 2014; Revised 24 September 2014; Accepted 24 September 2014

Abstract

Nutrient transporters are critical gate-keepers of extracellular metabolite entry into the cell. As integral membrane proteins, most transporters are *N*-glycosylated, and the *N*-glycans are remodeled in the Golgi apparatus. The Golgi branching enzymes *N*-acetylglucosaminyltransferases I, II, IV, V and avian VI (encoded by Mgat1, Mgat2, Mgat4a/b/c Mgat5 and Mgat6), each catalyze the addition of *N*-acetylglucosamine (GlcNAc) in *N*-glycans. Here, we asked whether *N*-glycan branching promotes nutrient transport and metabolism in immortal human HeLa carcinoma and non-malignant HEK293 embryonic kidney cells. Mgat6 is absent in mammals, but ectopic expression can be expected to add an additional β1,4-linked branch to *N*-glycans, and may provide evidence for functional redundancy of the *N*-glycan branches. Tetracycline (tet)-induced overexpression of Mgat1, Mgat5 and Mgat6 resulted in increased enzyme activity and increased *N*-glycan branching concordant with the known specificities of these enzymes. Tet-induced Mgat1, Mgat5 and Mgat6 combined with stimulation of hexosamine biosynthesis pathway (HBP) to UDP-GlcNAc, increased cellular metabolite levels, lactate and oxidative metabolism in an additive manner. We then tested the hypothesis that *N*-glycan branching alone might promote nutrient uptake when glucose (Glc) and glutamine are limiting. In low glutamine and Glc medium, tet-induced Mgat5 alone increased amino acids uptake, intracellular levels of glycolytic and TCA intermediates, as well as HEK293 cell growth. More specifically, tet-induced Mgat5 and HBP elevated the import rate of glutamine, although transport of other metabolites may be regulated in parallel. Our results suggest that *N*-glycan branching cooperates with HBP to regulate metabolite import in a cell autonomous manner, and can enhance cell growth in low-nutrient environments.

Key words: Golgi *N*-glycan branching, hexosamine biosynthetic pathway, metabolism, *N*-acetylglucosaminyltransferase enzymes, nutrient uptake

Introduction

The *medial* Golgi *N*-acetylglucosaminyltransferases I, II, IV and V (Mgat1, Mgat2, Mgat4a/b/c and Mgat5) form a linear pathway that initiates the *N*-acetylglucosamine (GlcNAc) branches on newly synthesized glycoproteins (Figure 1A) (Schachter 1986). In the *trans*-Golgi enzymes, the branches are extended with galactose, fucose and sialic acid to generate sequences recognized by galectins, C-type lectins and siglecs. The *N*-glycan branching pathway is required for tumor progression, and molecular mechanisms have emerged that intersect with basic metabolism (Lau et al. 2007; Shirato et al. 2011). Tumor growth rates are reduced in Mgat5$^{-/-}$ mice with a polyomavirus middle T transgene or in Pten heterozygous mice (Granovsky et al. 2000; Cheung and Dennis 2007;). Suppression of branching by either Mgat1 shRNA (Beheshti-Zavareh et al. 2012) or overexpression of *N*-acetylglucosaminyltransferase III (Yoshimura et al. 1995; Song et al. 2010) also inhibit tumor progression in mice. Furthermore, overexpression of Mgat5 in epithelial cells promotes transformation (Demetriou et al. 1995), and in human mammary and colon cancer, increased Mgat5-branched *N*-glycans are associated with disease progression (Fernandes et al. 1991; Seelentag et al. 1998).

We have shown that galectins bind branched *N*-glycans and cross-link glycoprotein to form a highly dynamic lattice that slows loss of membrane glycoproteins to endocytosis (Lau and Dennis 2008). In Mgat5$^{-/-}$ tumor cells, the retention of surface receptors is reduced along with sensitivity to cytokines (EGF, PDGF, INS and TGF-β). The mutant phenotype could be rescued by (i) Mgat5 re-expression, (ii) inhibition of constitutive endocytosis or (iii) increased uridine-diphosphate-*N*-acetylglucosamine (UDP-GlcNAc), the common nucleotide-sugar donor for the Mgat enzymes (Partridge et al. 2004; Lau et al. 2007). In the absence of Mgat5, compensating amounts of *N*-acetyllactosamine branches are produced by Mgat1, Mgat2 and Mgat4 when cells are supplemented with GlcNAc to increase UDP-GlcNAc (Lau et al. 2007). This suggests redundancy of the branches and cooperative action of *N*-glycans in support of growth factor receptors and other glycoproteins at the cell surface (Dennis and Brewer 2013). Interestingly, the chicken (*Gallus gallus*) GnT-VI (Mgat6) enzyme catalyzes the GlcNAcβ1,4 linkage to GlcNAcβ1,6Manα1,6Manβ in the trimannosyl core of *N*-glycans (Figure 1A). Mgat6 is expressed widely in birds (Watanabe et al. 2006), with homologs in frog (*Xenopus laevis*), duck billed platypus (*Ornithorhynchus anatinus*) and a few species of fish. The Mgat6 sequence is unrelated to Mgat4a/b/c. Mgat6 gene and activity are absent in mammals, suggesting the gene was selectively retained in certain species. If *N*-glycan branching is indeed cooperative and regulates metabolism, we predict that ectopic expression of Mgat6 in mammalian cells may reveal evidence for both.

Growth factor receptors activate Akt, Ras and mTor/S6K signaling, which leads to increased glucose (Glc) and amino acid transporter activity (Frauwirth et al. 2002; Wise et al. 2008; Yun et al. 2009; Wellen et al. 2010). Many of the ~600 mammalian solute transporters have extracellular domains with sites of *N*-glycosylation, and like receptor kinases, may be regulated by *N*-glycan branching. Glc transporters (Gluts) are dependent on *N*-glycan branching for surface residency of Glut2 in β-cells (Ohtsubo et al. 2005), Glut1 in tumor cells (Kitagawa et al. 1995) and insulin- or HBP-stimulated increases in surface Glut4 (Lau et al. 2007; Haga et al. 2011). The GlcNAc β1,4-branching enzyme GnT-IVa (Mgat4a) is selectively expressed in insulin-producing β cells of the pancreas, and Mgat4a$^{-/-}$ mice develop type 2 diabetes (Ohtsubo et al. 2005; Takamatsu et al. 2010). The branched *N*-glycans on Glut2 bind galectin-9 which promotes surface residency of Glut2, and transport of Glc.

N-Glycan branching depends on *de novo* synthesis of UDP-GlcNAc by the hexosamine biosynthesis pathway (HBP) and/or salvage of GlcNAc. Moreover, growth factor signaling increases UDP-GlcNAc levels, and shRNA inhibition of glutamine:fructose-6P aminotransferase in the *de novo* HBP-reduced Ras-driven tumor growth (Ying et al. 2012). Ras/Mapk and PI3K signaling also stimulates Mgat5 gene expression (Dennis et al. 1989; Kang et al. 1996; Buckhaults et al. 1997), as well as Mgat4 in human carcinomas (Takamatsu et al. 1999; D'Arrigo et al. 2005). The affinity of Mgat1, Mgat2, Mgat4a/b/c and Mgat5 enzymes for UDP-GlcNAc decreases ~400-fold moving from Mgat1 to Mgat5. As such, Mgat1 functions near saturation and Mgat5 well below its Km value for UDP-GlcNAc (i.e., ~10 mM) (Sasai et al. 2002; Lau et al. 2007). The action of Mgat1 is required to generate substrates for further remodeling by α-Mannosidase II, Mgat 2, Mgat4 and Mgat5. Glutamine (Gln) supplied to cells above typically used cell culture levels (>4 mM) increases UDP-GlcNAc levels, similar to GlcNAc supplementation in normal culture conditions, while Glc below physiological concentration (<5 mM) reduced UDP-GlcNAc levels (Abdel Rahman et al. 2013). Thus both Glc and Gln flux through HBP regulate UDP-GlcNAc levels, but at the low and high end of their concentration ranges, respectively. These studies offer the intriguing possibility that cellular regulation of *N*-glycan branching on solute transporters and receptors has evolved as a mechanism of adaptation to changing nutrient and environmental cues.

Mgat5-deficient mice are hypoglycemic, hyposensitive to glucagon (Johswich et al. 2014) and resistant to weight-gain on a high-fat diet, although their food intake is equivalent to wild-type littermates (Cheung et al. 2007). This suggests that *N*-glycan branching may promote a "thrifty phenotype", that is, efficiency in uptake and/or utilization of nutrients (Cheung et al. 2007). As an experimental model, we generated HeLa tumor cells and HEK293 immortalized cells with inducible transgenes for Mgat1, Mgat5 or Mgat6 overexpression. Here, we have characterized the effects of short-term (24 h) transgene overexpression on nutrient levels and central metabolism in cells. We report that Mgat1, Mgat5 and Mgat6 overexpression alone, and with HBP stimulation to UDP-GlcNAc, increases metabolite levels, suggesting cooperative action of the *N*-glycan-branching enzymes. Mgat5 transgene overexpression alone restored metabolite levels and HEK293 cell growth to normal in low Gln and Glc culture conditions. The uptake rate of Gln and the intracellular levels of other amino acids were enhanced by Mgat5 overexpression. This is the first evidence of cell autonomous regulation of nutrient uptake and metabolism by *N*-glycan branching.

Experimental procedures

Materials

Antibodies to FLAG-M2 and tubulin were purchased from Sigma-Aldrich. Alexa Fluor-488 conjugated lectins Concanavalin A (ConA) and leucoagglutinin (L-PHA) were purchased from (Invitrogen). Metabolite standards and reagents were obtained from Sigma Chemicals (St. Louis, MO) with minimal purity of 98%. Stable-isotope $^{15}N^{15}N$-L-Gln was purchased from Cambridge Isotope Laboratories, Inc. (Andover, MA). All organic solvents and water used in sample and LC–MS mobile phase preparation were HPLC grade and obtained from Fisher Scientific (Fair Lawn, NJ). *N*-Glycosidase F (PNGase F, EC 3.5.1.52, recombinant cloned from *Flavobacterium meningosepticum* and expressed in *Escherichia coli*) was purchased from Roche Diagnostics (Mannheim, Germany). PVDF membrane

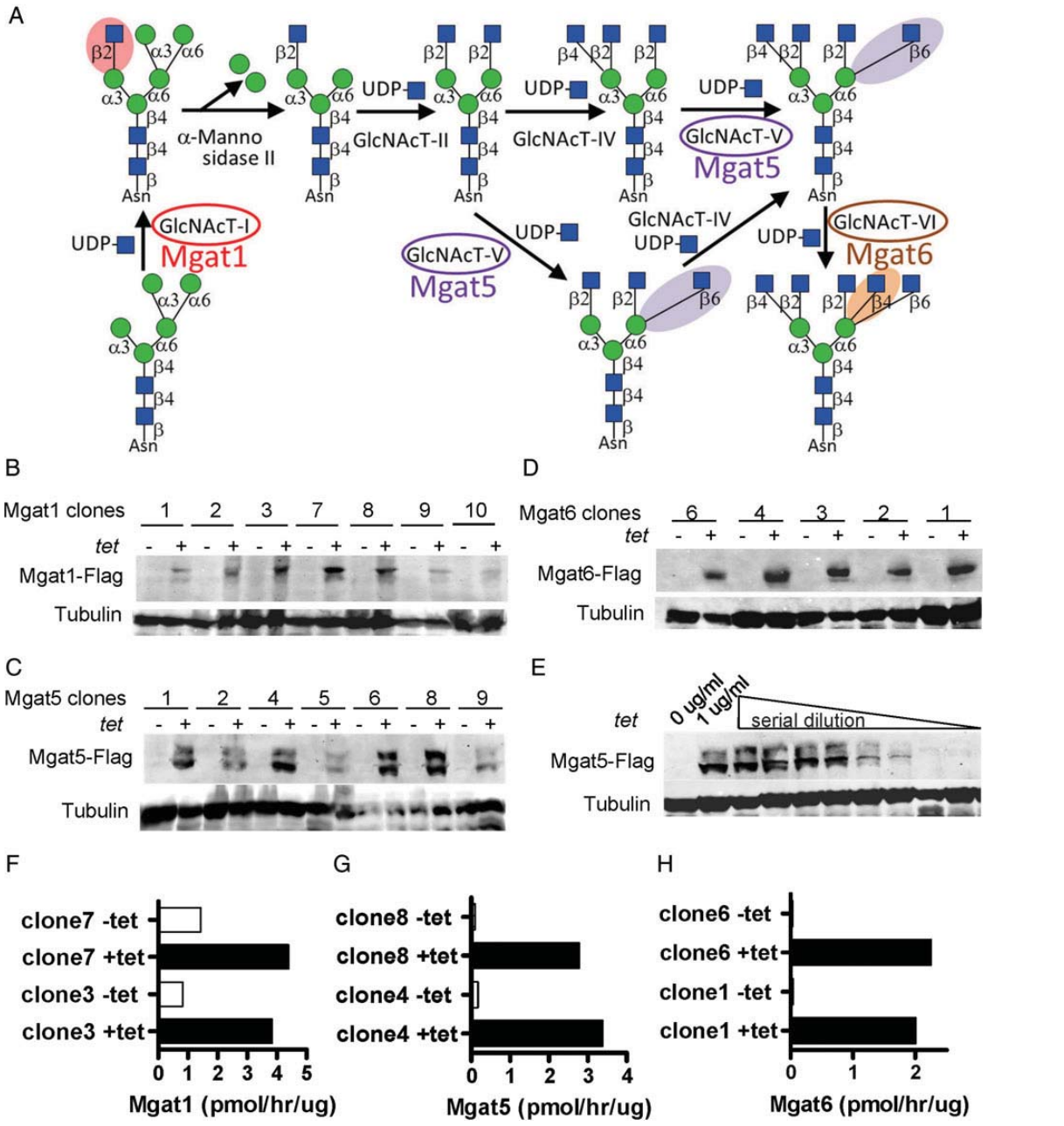

Fig. 1. Branching pathway and inducible expression of branching enzymes. (**A**) *N*-Glycan-branching pathway modified from Varki et al. (2009). GlcNAcT-I (Mgat1), GlcNAcT-V (Mgat5) and avian GlcNAcT-VI (Mgat6) are circled. (**B–D**) Expression of transgene proteins detected by western blots probed with antibodies to Flag and tubulin. Flag-tagged GlcNAcT-I, GlcNAcT-V (upper band) and GlcNAcT-VI have expected molecular weights of 53, 86 and 54 kDa, respectively. Flp-In-TREx HeLa clones were cultured in DMEM with 25 mM Glc, 4 mM Gln, 10% FBS (normal culture conditions), with or without 1 μg/mL of tet for 24 h. (**E**) Tet dose–response in clone 8 Mgat5 Flp-In-TREx HeLa cells. (**F–H**) *N*-Acetylglucosaminyltransferases activities measured in cell lysates from tet-inducible expression of Flag-tagged Mgat1, Mgat5 and Mgat6 in different Flp-In-TREx HeLa cell clones.

(Immuno-Blot, 0.2 μm, 7.0 × 8.5 cm) was purchased from Bio-Rad (Hercules, CA). Cation-exchange columns were made of (30 mg) Dowex 50W-X8 200-400 mesh resins (Wako Chemical, Osaka, Japan) packed on top of a 10 μL ZipTip u-C18 (Millipore, Billerica, MA). The resins were protonated with 1 M HCl (50 μL, 3 times), were rinsed with methanol (50 μL, 3 times), and then equilibrated with water (50 μL, 3 times) before use. Microtiter plates (96-well flat bottom, MaxiSorp) were purchased from Nunc (Roskilde, Denmark). All other chemicals were purchased from Sigma-Aldrich, Nacalai Tesque (Kyoto, Japan) or Wako Chemical. Other reagents and solvents were of HPLC or LC–MS grade.

Cell lines

HeLa Flp-In-TREx cells were a kind gift from Dr Stephen Taylor (University of Manchester), while HEK293 Flp-In-TREx cells (Ward et al.

2011) were purchased from Invitrogen. Both adherent cell lines were grown in an incubator at 37°C and 5% CO_2 in a humidified atmosphere. They were maintained in high-Glc DMEM (Sigma) supplemented with 10% fetal bovine serum (FBS), 2 mM Gln, penicillin/streptomycin, and 3 μg/mL Blastocidin and 100 ug/mL Zeocin, unless indicated otherwise. Human Mgat1 cDNA, human Mgat5 cDNA and chicken Mgat6 cDNA were FLAG tagged at the N terminus, and each construct was cloned individually into the pcDNA5/FRT/TO expression vector. Each plasmid was integrated into the genome of the HeLa or HEK293 Flp-In-TREx cells, at a pre-integrated FRT recombination site, by co-transfection with Flp recombinase encoding POG44 plasmid using Lipofectamine (Invitrogen) and OptiMEM media lacking FBS or antibiotics. Following selection in 200 μg/mL of hygromycin, resistant clones were individually picked, expanded and treated with 1 μg/mL tetracycline (tet) for 24 h. To verify gene expression, cell lysates were analyzed by western blotting using monoclonal Anti-FLAG M2 antibody (Sigma).

Western blotting

Cells were rinsed with ice-cold phosphate-buffered saline (PBS) and lysed in ice-cold lysis buffer (50 mM HEPES, 120 mM NaCl, 2 mM EDTA, 1.0% NP-40, one tablet of phosphatase inhibitor cocktail per 10 mL and one tablet of EDTA-free protease inhibitors per 10 mL). The soluble fractions of cell lysates were isolated by centrifugation at 14,000 rpm for 10 min by centrifugation in a microfuge at 4°C. Proteins were denatured by addition of 5× sample buffer, boiled for 5 min, resolved by 8 or 10% SDS–PAGE and analyzed by immunoblotting for the FLAG-tagged proteins.

Enzyme assays

Enzyme sources were cell lysates obtained from large plates of tet-induced and not induced cells lysed on ice in 0.9% NaCl, 1% Triton X-100, and including protease inhibitors (Korczak et al. 2000; Beheshti Zavareh et al. 2012). Mgat1 enzyme activity was measured using synthetic acceptors. The assays contained 10 μL of cell lysate, 2 mM Man(1,3) Man(1,6) Glc-O$(CH_2)_7CH_3$ acceptor (Toronto Research Chemicals), 0.5 μCi [6-^{3}H]-UDP-GlcNAc (44,400 dpm/nmol) in 50 mM MES, pH 6.5, 2 mM Mn_2Cl_2, 5 mM AMP in total volume of ~20 μL. After 1.5 h of incubation at 37°C, 1 mL of ice-cold water was added to stop further reaction and assays were either frozen or processed immediately. Mgat5 enzyme activity was determined as transfer of UDP-[6-^{3}H] GlcNAc to the synthetic acceptors. The reaction contained 10 μL of cell lysate, 1 μCi of [6-^{3}H]-UDP-GlcNAc (44,000 dpm/nmol), 50 mM MES, pH 6.5, 0.5 M GlcNAc, 1 mM UDP-GlcNAc, 1 μCi of ^{3}H-UDP-GlcNAc, 25 mM AMP, in a final volume of 20 μL, with synthetic acceptors 1 mM βGlcNAc(1,2)αMan(1,6)βGlc-O$(CH_2)_7CH_3$ for Mgat5. Reactions were incubated at 37°C for 180 min for the Mgat5 assay. Endogenous activity for the enzymes was measured in the absence of acceptor, and subtracted from values determined in the presence of added acceptor. Reactions were stopped with 1 mL of H_2O, and enzyme products were separated from radioactive substrates by binding them to 50 mg C_{18} cartridges (Alltech), preconditioned with methanol rinsing and water washes. Reactions were loaded and the columns washed three times with water. Radio-labeled products were eluted with methanol directly into scintillation vials with two separately applied 250 μL aliquots of methanol, and the radioactivity determined by liquid scintillation counting.

Mgat6 enzyme activity was assayed according to the method of Taguchi et al. (2000) using as acceptor substrate, PA-agalacto [(2,6),(2,4)] tetra-antennary and 100 mM UDP-GlcNAc in buffer 150 mM HEPES-NaOH, 60 mM $MnCl_2$, 200 mM GlcNAc, 0.5% Triton X-100 and 2 mg/mL BSA for 4 h at 37°C. The product was separated by HPLC on TSKgel ODS-80TM (0.46 × 15 cm, Tosoh, Tokyo, Japan), eluted with 20 mM ammonium acetate (pH 4.0)/0.02% 1-butanol at flow rate of 1 mL/min, column temp at 55°C and detection by fluorescence (excitation/emission = 320/400 nm)

Quantitative lectin fluorescence imaging

Cells were plated in a 96-well plate at 2000 cells/well in high-Glc DMEM supplemented with 10% FBS, 2 mM Gln and incubated at 37°C and 5% CO_2 with and without tet for 24 h to induce gene expression. Cells were then fixed for 15 min with 4% paraformaldehyde, washed with PBS and incubated for 1 h at room temperature in 50 μL PBS, 1/5000 of Hoechst 33342, and either 1/1000 of 2 mg/mL Alexa Fluor-488 conjugated lectin ConA or L-PHA (Invitrogen, Carlsbad, CA). After washing with PBS, cells were imaged and staining per cell quantified using IN Cell Analyzer 1000 automated fluorescence imaging system.

Cell viability assay

Following plating in a 96-well cell culture plate, and treatment with various concentrations of Glc, Gln and FBS in DMEM for at least 24 h, AlamarBlue cell viability reagent (Invitrogen) was added at one-tenth of the volume directly to cells in cell culture media. The plate was then returned to the incubator at 37°C and 5% CO_2 in a humidified atmosphere for an additional incubation of 6 h. Cell viability was measured fluorometrically, as relative fluorescence units, in a microplate reader (Gemini Fluorescence from Molecular Devices) following the reduction of the non-fluorescent oxidized dye AlamarBlue by viable and metabolically active cells to its fluorescent product, using fluorescent excitation and emission wavelengths of 570 and 585 nm, respectively. The number of metabolically active, proliferating, viable cells correlates with the magnitude of dye reduction and fluorescence emission intensity from each well.

Cell membrane preparation for *N*-glycan profiling

For *N*-glycan analysis by LC–MS, HeLa and HEK293 Flp-In-TREx cells were cultured in standard culture medium, DMEM plus 10% FBS at 37°C and 5% CO_2 in a humidified atmosphere for 24 h, with and without 1 μg/mL tet to induce gene expression. Approximately 2×10^7 cells per treatment were rinsed with PBS, trypsinized, collected in pellets, frozen on dry ice and stored at −80°C. The frozen pellets were suspended in 2 mL of lysis buffer containing 50 mM Tris–HCl (pH 7.4), 0.1 M NaCl, 1 mM EDTA and protease inhibitor cocktail (Roche Diagnostics, Mannheim, Germany) and kept on ice for 20 min and then homogenized using a polytron homogenizer (Omni TH tissue homogenizer, Omni International, Inc., VA; 15 s, 7 times on ice bath). We performed the following preparation according to the procedure reported by Nakano et al. (2011) with some modifications. The homogenized cells were centrifuged at 2000 × *g* for 20 min at 4°C to precipitate nuclei and unlyzed cells. The supernatant was diluted with 2 mL of Tris-buffer (50 mM Tris–HCl, pH 7.4, 0.1 M NaCl) and then were sedimented by ultracentrifugation at 120,000 × *g* for 80 min at 4°C (swing rotors, Himac, Hitachi Koki). The supernatant was discarded, and the membrane pellet was

suspended in 100 µL Tris-buffer. After adding 400 µL Tris-buffer containing 1% (v/v) Triton X-114, the suspended mixture was homogenized by pipetting strongly. The homogenate was chilled on ice for 10 min and incubated at 37°C for 20 min and then phase partitioned by centrifugation at 1940 × *g* for 2 min. The upper aqueous phase was removed. The lower detergent phase was further mixed with 1 mL of ice-cold acetone and kept at −25°C overnight to precipitate proteins and remove any detergent. After centrifugation at 1940 × *g* for 2 min, the precipitated cell membrane proteins were stored at −25°C if not used immediately.

Enzymatic release and purification of *N*-glycans

The precipitated membrane proteins were dissolved with 10 µL 8 M urea. The solubilized proteins were dotted (2.5 µL × 4 times) onto PVDF membrane prewetted with ethanol. After drying the PVDF membrane with cold blast of a dryer for 10 min, the PVDF membrane was rinsed with ethanol for 1 min and then rinsed three times for 1 min with water. The protein on the membrane was stained for 5 min with (800 µL solution A: 0.1% (w/v) Direct Blue 71 (Sigma-Aldrich) in 10 mL solution B : acetic acid : ethanol : water = 1 : 4 : 5). After destaining with solution B for 1 min, the PVDF membrane was dried with cold blast of a dryer for 10 min. Protein stained blue was cut from the PVDF membrane and placed in separate wells of a 96-well microtiter plate. The spots were then covered with 100 µL of 1% (w/v) polyvinylpyrrolidone 40,000 in 50% (v/v) methanol, agitated for 20 min and rinsed with water (100 µL × 5 times). PNGase F (3 U in 10 µL of 30 mM phosphate buffer, pH 7.3) was added to each well and incubated at 37°C for 15 min. An additional 10 µL of water was added to each well and incubated at 37°C overnight to release *N*-glycans. During the incubation, the sample wells were sealed with amplification tape to prevent evaporation. To collect the released *N*-glycans, the samples were sonicated (in the 96-well plate) for 10 min, and the released *N*-glycans (20 µL) were transferred to 1.5 mL polypropylene tubes. The sample well was rinsed with water (50 µL twice), and the washings combined. To completely generate the reducing terminus, ammonium acetate buffer (100 mM, pH 5.0, 20 µL) was added to the released *N*-glycans for 1 h at room temperature. After evaporating to dryness, the glycans were resolved with 10 µL of 50 mM KOH and then reduced by adding 10 µL of 2 M $NaBH_4$ in 50 mM KOH at 50°C for 3 h. one microliter of acetic acid was added to stop the reaction, and the *N*-glycan alditols were desalted using a cation-exchange column. The glycan alditols were eluted with water (50 µL twice), dried, and the remaining borate was removed by the addition of (100 µL × 3) methanol and drying under vacuum. To remove sialic acids from the glycans, 100 µL of 2 M acetic acid was added to the dried glycan samples and the samples were incubated at 80°C for 2 h and then were evaporated to dryness. The desialylated *N*-glycan alditols were re-suspended in 10 mM NH_4HCO_3 (20 µL) immediately before glycan analysis by liquid chromatography–electrospray ionization mass spectrometry (LC–ESI-MS).

LC–ESI-MS for analysis of *N*-glycan alditols

N-Glycan alditols were separated using a HyperCarb porous graphitized carbon column (5 µm HyperCarb, 0.32 mm ID × 100 mm, Thermo Scientific) under the following gradient conditions. The separation was performed using a sequence of isocratic and two segmented linear gradients: 0–8 min, 10 mM NH_4HCO_3; 8–53 min, 6.75–15.75% (v/v) CH_3CN in 10 mM NH_4HCO_3; 53–73 min, 15.75–40.5% (v/v) CH_3CN in 10 mM NH_4HCO_3; and increasing to 81% (v/v) CH_3CN in 10 mM NH_4HCO_3 for 6 min and re-equilibrated with 10 mM NH_4HCO_3 for 15 min at a flow rate of 5 µL/min (LC/MSD Trap XCT Plus Series 1100, Agilent Technologies). The injection volume of samples was 5 µL. In the MS (Esquire HCT, Bruker Daltonics GmbsH, Bremen, Germany), the voltage of the capillary outlet was set at 3.5 kV, and the temperature of the transfer capillary was maintained at 300°C. The flow rate of nitrogen gas for drying was 5 L/min. The MS spectra were obtained in the negative ion mode over the mass range *m/z* 150–3000. The scan rates were 8100 a.m.u./s for the MS mode and the MS/MS mode. Monoisotopic masses were assigned with possible monosaccharide compositions using the GlycoMod tool available on the ExPASy server (http://au.expasy.org/tools/glycomod; mass tolerance for precursor ions is ±0.1 Da), and the proposed oligosaccharide structures were provided at UnicarbKB database (http://unicarbkb.org/), and further verified through annotation using a fragmentation mass matching approach based on the MS/MS data. Validation of the technical reproducibility of the analytical conditions such as retention time and mass number was carried out using known glycans derived from bovine fetuin before analyzing any experimental samples. The relative abundance of each glycan structure on the cell membrane glycoproteins was calculated based on the peak area of the ion chromatogram of the corresponding glycan structure extracted using the mass of the $[M-2H]^{2-}$ ion (width 1.0 Da, e.g., 893.3–894.3 for structure (1) in Supplementary data, Figure S1), after processing of the peaks (smoothing algorithm; Gauss, smoothing widths; 1 pnts, S/N thresholds; 1, no exclusion mass, using Bruker Daltonics DataAnalysis software ver. 3.4) (Nakano et al. 2011).

Metabolite analysis by LC–MS/MS

To determine the relative levels of metabolites, HeLa and HEK293 Flp-In-TREx cells were cultured in 6-well plates at 37°C and 5% CO_2 in a humidified atmosphere for 24 h in various nutrient conditions as described Abdel Rahman et al. (2013), with and without tet to induce gene expression. Media was aspirated and cells rinsed on the plates with warm PBS. The plates were snap frozen in liquid N2 and moved to −80°C until extraction. The metabolites were rapidly extracted by addition of 1 mL ice-cold solution of (40% acetonitrile, 40% methanol and 20% water). After quenching, the cells were scraped and transferred to 1.5 mL tube and shaken for 1 h at 4°C and 1000 rpm in a Thermomixer (Eppendorf, Germany). The samples were spun down at 14,000 rpm, for 10 min at 4°C (Eppendorf, Germany), and then the supernatant transferred to fresh tubes to be evaporated to dryness in a CentreVap concentrator at 40°C (Labconco, MO). The dry extract samples were stored at −80°C for LC–MS analysis. Cell number for each culture condition was determined for normalization purposes by trypsinization of parallel replicate wells. The dry metabolite extracts were reconstituted in 200 µL of water containing internal standards (500 and 300 µg/mL of D_7-Glc and $^{13}C_9^{15}N$-Tyrosine, respectively), for the purpose of calibration, normalization and quantification. The mixture of metabolites was injected twice through the HPLC (Dionex Corporation, CA) in gradient reversed phase column Inertsil ODS-3, 4.6 mm internal diameter, 150 mm length and 3-µM particle size for positive and negative mode analysis. In positive mode analysis, the mobile phase gradient ramps from 5 to 90% of acetonitrile in 16 min, then after 1 min at 90%, the composition returns to 5% acetonitrile in 0.1% acetic acid in 2 min. In negative mode, the acetonitrile composition ramped from

5 to 90% in 10 min, then after 1 min at 90%, the gradient ramped back to 5% acetonitrile in buffer A (0.1% tributylamine, 0.03% acetic acid and 10% methanol). The total runtime in both modes was 20 min, the samples were stored at 4°C, and the injection volume was 10 µL. An automated washing procedure was developed before and after each sample to avoid any sample carryover.

The eluted metabolites were analyzed at the optimum polarity in multiple reaction monitoring (MRM) mode on electrospray ionization (ESI) triple-quadrupole mass spectrometer (ABSciex4000Qtrap, Toronto, ON, Canada) (Abdel Rahman et al. 2014). The mass spectrometric data acquisition time for each run is 20 min, and the dwell time for each MRM channel is 10 ms. Common mass spectrometric parameters are the same as tuning conditions, except: GS1 and GS2 were 50 psi; curtain gas (CUR) was 20 psi, and CAD was 3 and 7 for positive and negative modes, respectively, and source temperature (TEM) was 400°C. Signal was normalized to internal standard and cell number. The LC–MS/MS system does not resolve hexose, hexosamine and nucleotide sugar stereoisomers, including Glc/Galactose, GlcNAc/GalNAc, GlcNAc-6P/GlcNAc-1P and UDP-GlcNAc/UDP-GalNAc. To monitor trends in metabolic pathways, we referred to these stereoisomers in their Glc forms.

Stock solutions were prepared for each metabolite standard at a concentration of 100 µM in 40/60 methanol/water (v/v), 0.1% NaOH. A final concentration (10 µM) of each metabolite was obtained for mass spectrometric tuning. A standard mixture of all metabolites was prepared at 200, 500 and 3000 nM as a sensitivity and specificity quality control. Ten additional serially diluted samples were prepared ranging from 1 nM to 2 µM for linearity assessments. A mixture of all the standard metabolites was used daily to check the LC–MS/MS system for optimal ionization polarity, declustering potential, precursor ion (Q1), product ion (Q3) and collision energy. Ion source potential was 4500 V for positive and negative modes. Nebulizer gas (GS1) and bath gas (GS2) were 10 psi, CUR was 15 psi, and collision gas (CAD) was 4 psi. Source temperature (TEM) was set to zero and interface heater was ON. The mass spectrometer was maintained and calibrated using a special kit designed by the manufacturer (ABSciex, Toronto, ON, Canada).

The raw LC–MS/MS data were imported to MultiQuant version 2.0.0 (ABSciex) and the extracted ion chromatogram peaks were integrated. The result table contains the area, area ratio (area of analyte/area of internal standard), retention time and concentration, and is then exported from MultiQuant as text files to MarkerView version 1.2.11 (ABSciex) for normalization with cell number and protein content. Cell number normalized data were analyzed using the MetaboAnalyst online software for metabolomic analysis (http://www.metaboanalyst.ca/MetaboAnalyst/), and the KEGG databases (http://www.genome.jp/kegg/pathway.html) (Xia et al. 2012).

LC–MS/MS measurement of $^{15}N^{15}N$-Gln uptake and metabolism

Flp-In-TREx HEK293 Mgat5 cells were treated for ~24 h with 1 mg/mL of tet, to induce Mgat5 gene expression, in DMEM with 2.5 mM Glc and no Gln plus 10% FBS, with and without 15 mM GlcNAc. The media was then changed to DMEM with 2.5 mM Glc and 1 mM $^{15}N^{15}N$-Gln without FBS, for 1, 5 and 10 min. After incubation, cells were collected and metabolites extracted using the procedure detailed above. The chromatographic peaks for metabolite interest, and correct transitions for the labeled form of the metabolite were integrated using MultiQuant (ABSciex) (Soliman et al. 2014).

Results

Tet-inducible expression of Mgat1, Mgat5 and Mgat6 in human cells

To generate transgenic cell lines, HeLa and HEK293 cell lines with a single Flp-In-TREx insertion site were transfected with vectors for insertion of tet-inducible FLAG-tagged Mgat1, Mgat5 or Mgat6. The Flp-In-TREx site is designed for controlled expression from a single insertion, and indeed, tet-inducible expression of FLAG-tagged protein was detected in multiple-independent HeLa cell clones (Figure 1B–E). Independent clones displayed similar levels of tet-inducible expression, with increases in Mgat1 and Mgat5 enzyme activity by 4- and 30-fold, respectively, while Mgat6 introduced a novel activity not present in mammalian cells (Figure 1F–H). Changes in *N*-glycan composition at the cell surface were determined by ConA and L-PHA lectin staining. ConA binds *N*-glycans with two or fewer branches, and L-PHA binds Mgat5-modified tri- and tetra-antennary *N*-glycans. In HeLa cells, tet-induced Mgat1 enhanced Con A but not L-PHA binding. L-PHA binding was enhanced in tet-induced Mgat5, while ConA was unchanged (Figure 2A and B). Tet-induced Mgat6 reduced L-PHA binding suggesting the addition of the Mgat6 branch to Mgat5-branched *N*-glycans may interfere with L-PHA binding (Figure 2B).

To further characterize the tet-induced Mgat1, Mgat5 and Mgat6 changes in the *N*-glycan distributions, we released structures from Flp-In-TREx HeLa cell glycoproteins by PNGase and analyzed the *N*-glycan alditols by LC–ESI-MS. We interpret these data in light of the known specificity of the enzymes (Schachter 1986; Watanabe et al. 2006) and prior knowledge of the Golgi pathway in mammalian cells (Schachter 1986; Watanabe et al. 2006). We limited our interpretation to structures with the *N*-glycan core plus 1–4 Hex-HexNAc units, and the cartoon structures are drawn without branch linkages. The MS features corresponding to the masses of 16 predicted *N*-glycan structures were quantified, as shown by the examples in Supplementary data, Figures S2 and S3. Twenty-three additional structures are indicated by their *m/z* values and probable compositions (Figure 2C–E; Supplementary data, Figure S1). The profile for tet-induced Mgat1 HeLa cells revealed a 4- to 10-fold increase in the immediate product of Mgat1 (structures 14, 15 and 16) but not the down-stream tri- and tetra-antennary *N*-glycans (Figure 2C). This was consistent with the lectin-binding profile of the cells (Figure 2A and B), and suggests a backup in *N*-glycan processing due to insufficient α-mannosidase II activity. Tet-induced Mgat5 revealed a small increase in peaks with *m/z* of the expected products; 2,2,6 tri- and 4,2,2,6 tetra-antennary *N*-glycans with and without fucose (Figure 2D, structures 3, 5, 8 and 11). In tet-induced Mgat6 HeLa cells, novel peaks were observed with *m/z* predicted to be the 4,2,2,4 tetra- and 4,2,2,4,6 penta-antennary products of Mgat6 with and without fucose (Figure 2E). Structures 10, 12 and 13 are predicted to be tetra- and penta-antennary products of avian Mgat6, while the native 4,2,2,6 tetra-antennary *N*-glycans (structures 8 and 11) were reduced. This is consistent with our earlier studies showing that Mgat5-modified intermediates are the preferred acceptor for Mgat6 (Watanabe et al. 2006), thus conversion of tri- and tetra- to tetra- and penta-branched *N*-glycan (Figure 2E). Structures 8 and 11 are preferred ligands for L-PHA binding, and their conversion to 10, 12 and 13 is associated with reduced L-PHA binding (Figure 2B).

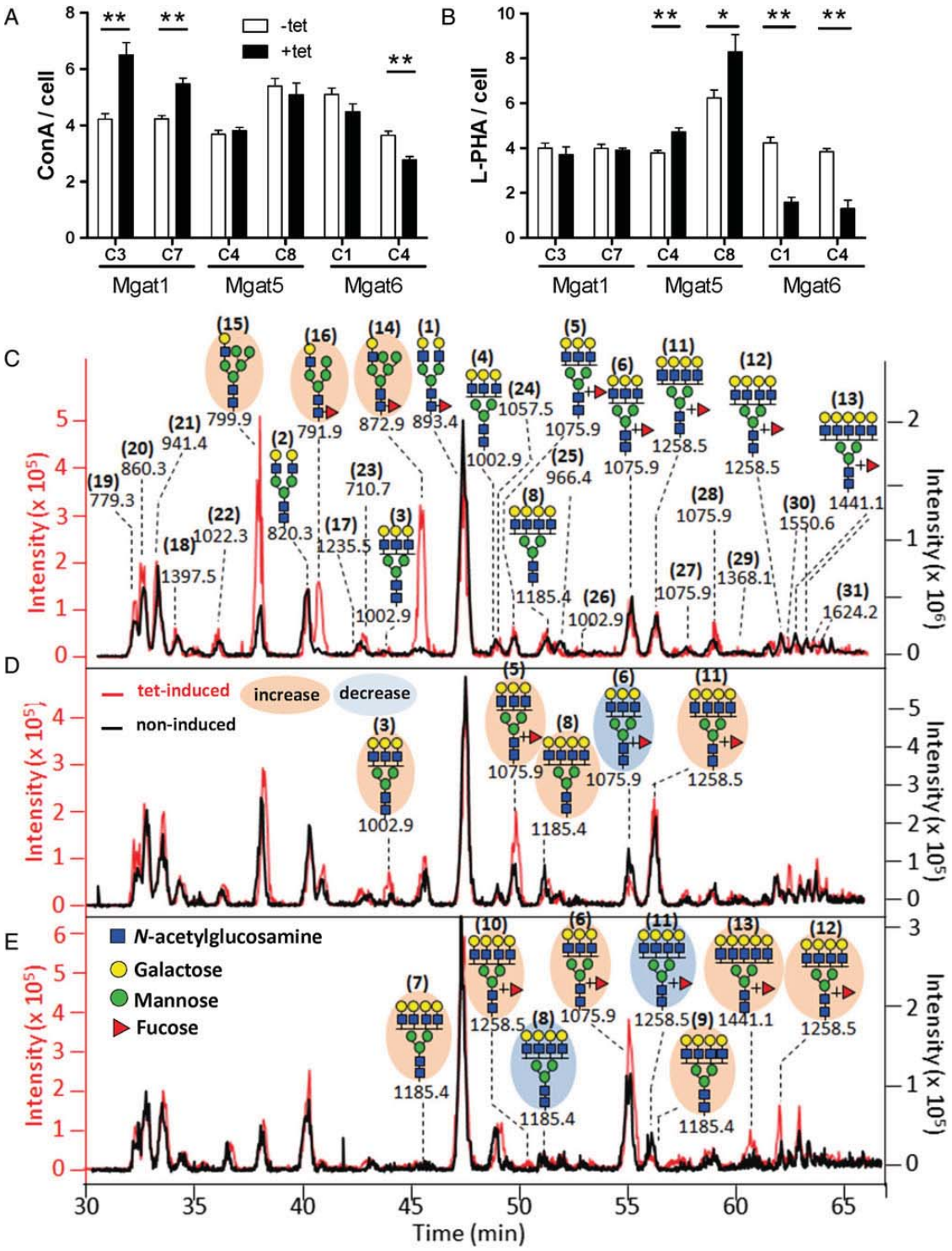

Fig. 2. *N*-Glycans profiles of transgenic Flp-In-TREx HeLa cells. (**A**) ConA and (**B**) L-PHA lectin binding to Mgat1, Mgat5 and Mgat6 in Flp-In-TREx HeLa clones, with and without 1 μg/mL tet for 24 h, measured by fluorescence microscopy, $*P < 0.05$ and $**P < 0.01$ by Student's *t*-test. (**C**–**E**) LC–ESI-MS chromatogram for *N*-glycans in Flp-In-TREx HeLa cells expressing (C) Mgat1 clone 3, (D) Mgat5 clone 8 and (E) Mgat6 clone 6. The red chromatogram is tet induced and black is non-induced. Yellow circles indicate increases, and blue circles indicate decreases. Cells were grown in DMEM, 25 mM Glc and 4 mM Gln + 10% FBS (standard conditions) with and without tet for 24 h.

A low amount of Mgat6 activity was detected in the absence of tet (Figure 1H), as well as a small amounts of structures 10, 12 and 13, suggesting some background (leaky expression) of the Mgat6 transgene (Figure 2E). HeLa cells had insufficient α-mannosidase II activity to process the tet-induced Mgat1 product (i.e., HexNAc-Hex_5-$HexNAc_2$-Asn), which appeared to be the limiting factor for tet-induced increases in Mgat5 and Mgat6 branched *N*-glycans.

Tet-inducible Mgat1, Mgat5 and Mgat6 *N*-glycan branching

HEK293 is an immortalized human embryonic cell line with epithelial morphology previously reported to be growth sensitive to changes in *N*-glycan branching and HBP (Lau et al. 2008). HEK293 cell lines with tet-inducible Mgat1, Mgat5 or Mgat6 were made by the Flp-In-TREx system, and displayed tet-inducible expression of the enzymes, comparable with that seen in the HeLa cell lines (Figure 3A; Supplementary data, Figures S2 and S3). Flp-In-TREx HEK293 clones also displayed very similar induction of enzyme activities and glycan branching, as illustrated for tet-inducible Mgat5 (Figure 3B). Tet-induced Mgat5 expression alone increased L-PHA binding by

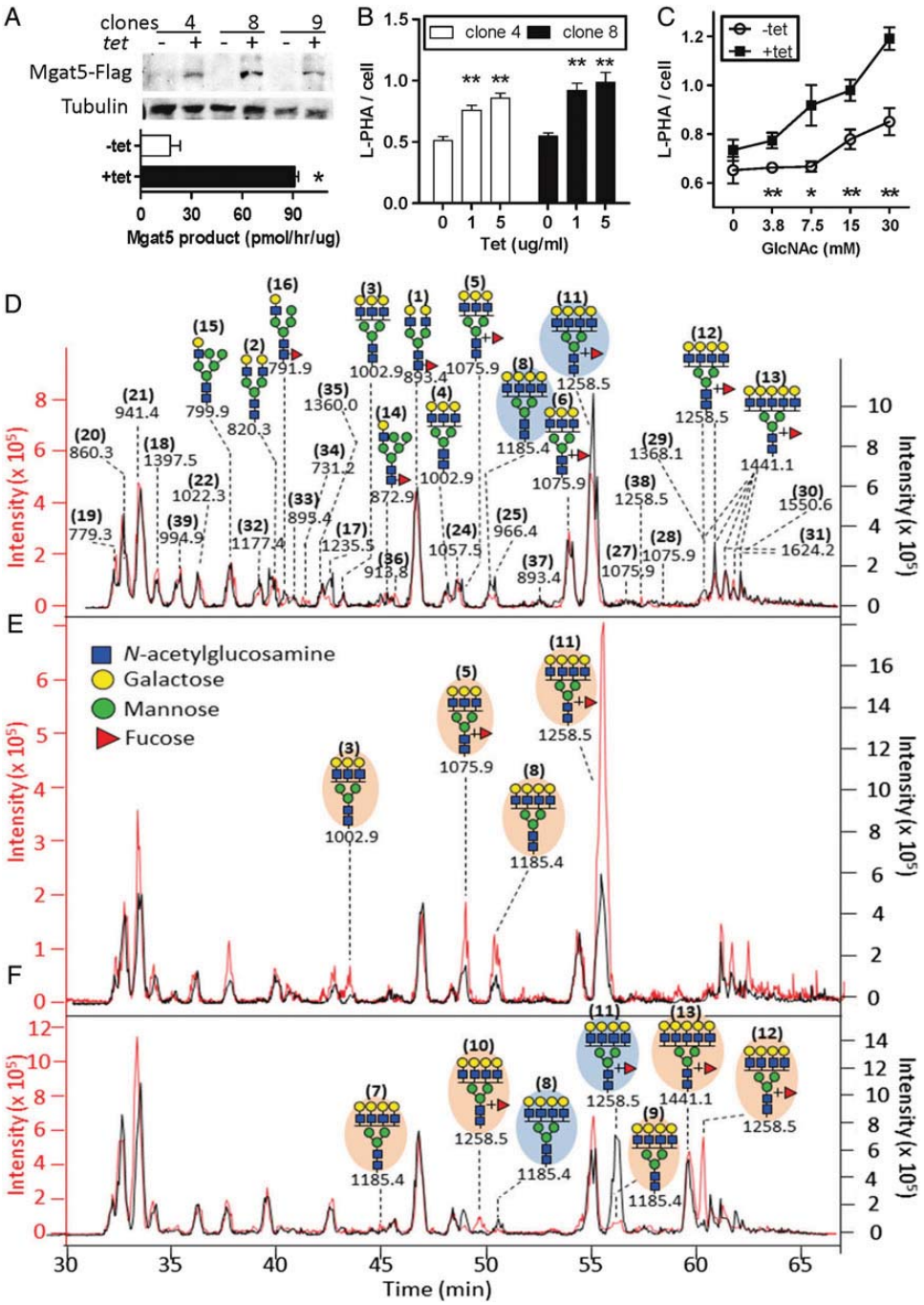

Fig. 3. *N*-Glycans profiles of transgenic Flp-In-TREx HEK293 cells by LC–ESI-MS. (**A**) Expression of transgene proteins detected by western blot probed with anti-Flag and tubulin antibodies in three different Flp-In-TREx Flag-tagged Mgat5 HEK293 clones, and Mgat5 enzyme activity measured in cell lysates from tet-inducible expression of Flag-tagged Mgat5 in clone 4. (**B**) Tet-induced Mgat5 increases complex-type *N*-glycan branching in HEK293 Mgat5 clones 4 and 8, quantified by Alexa-488 conjugated L-PHA fluorescence imaging. For quantification, mean ± SD, one-way ANOVA with Dunnett's multiple comparison test. (**C**) L-PHA binding of tri- and tetra-antennary *N*-glycans displays a synergistic effect for GlcNAc supplementation with tet-induced Mgat5 in clone 4. $*P<0.05$ and $**P<0.01$ by Student's *t*-test compared with tet control. (**D–F**) LC–ESI-MS chromatogram of *N*-glycans in Flp-In-TREx HEK293 cells expressing (D) Mgat1, (E) clone 4 Mgat5 and (F) Mgat6. Experimental conditions as described in Figure 2.

~13%, 30 mM GlcNAc supplementation to HBP by ~30%, and addition of both by ~83%, clearly displaying a synergistic interaction (Figure 3C).

To characterize the structural effects of tet-induction, *N*-glycans were released by PNGase and the *N*-glycan alditols were analyzed by LC–ESI-MS. Overall, HEK293 cells displayed a greater fold change

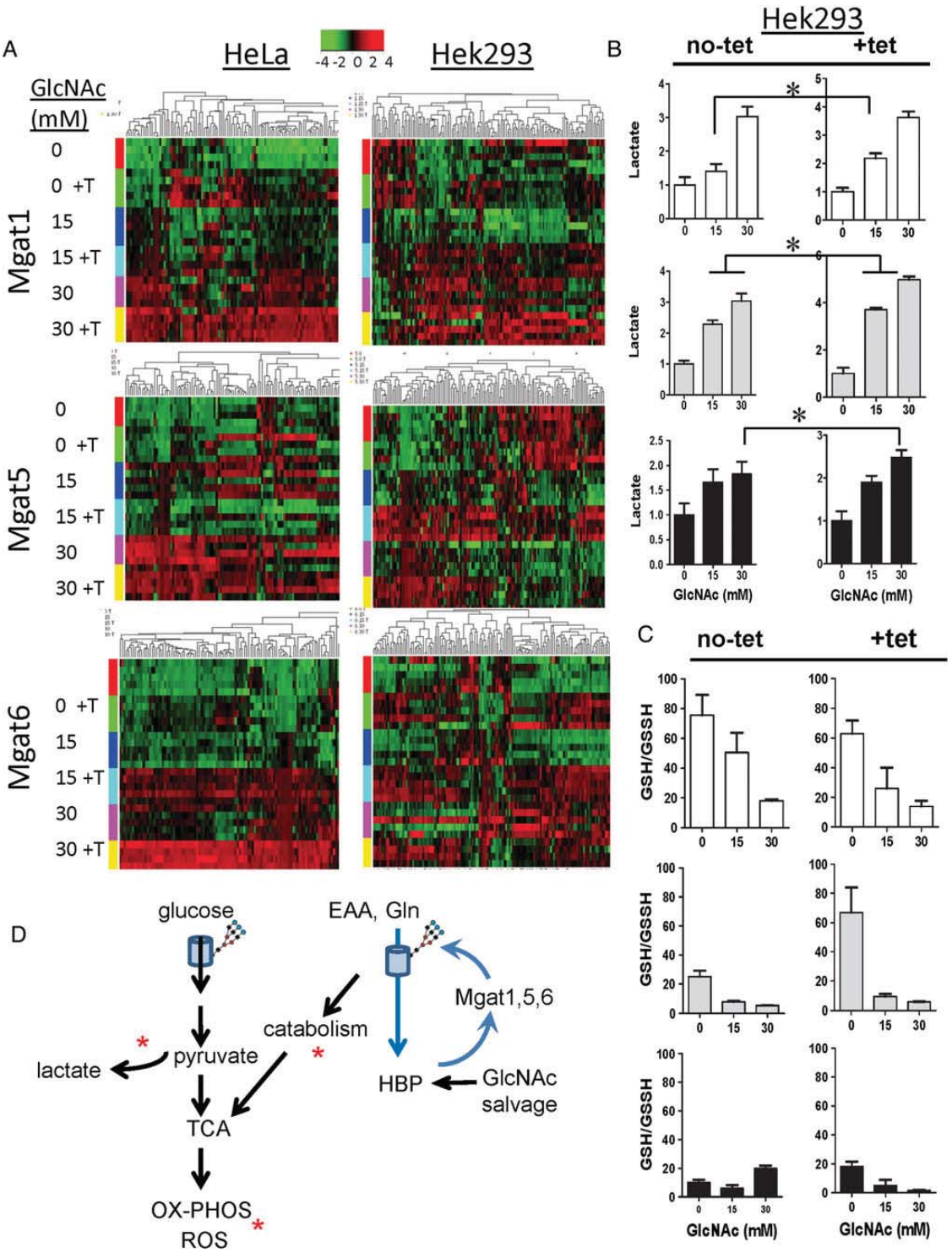

Fig. 4. Metabolite levels are sensitive to tet-induced branching and HBP stimulation. (**A**) Mgat1, Mgat5 and Mgat6 Flp-In-TREx HeLa and HEK293 cells were grown in standard culture conditions with and without tet (T) and 0, 15 or 30 mM GlcNAc supplementation for 24 h. Each row represents a biological replicate ($n = 4$–5). Metabolites in cell lysates were measured by targeted LC–MS/MS and normalized to cell number. Data for 129 metabolites were analyzed by unsupervised clustering and presented as heat maps (Supplementary data, Tables SII and SIII). (**B**) Lactate and (**C**) GSH/GSSG ratios in Flp-In-TREx HEK293 cells with and without tet-induced Mgat1, Mgat5 and Mgat6 induction for 24 h. Additive effects of tet and GlcNAc, $*P < 0.05$ by Student's *t*-test. (**D**) Scheme for increased nutrient uptake and flow to catabolism (*) with tet-induced increased *N*-glycan branching and GlcNAc supplementation. Blue arrows indicate putative positive feedback from central metabolism through de novo HBP to *N*-glycan branching.

in tri- and tetra-antennary *N*-glycans than HeLa cells (Figure 3D–F; Supplementary data, Figure S1). The tetra-antennary structures 8 and 11 were reduced in tet-induced Mgat1 HEK293 cells (Figure 3D). This may seem counter-intuitive, but is consistent with multistep ultrasensitivity to UDP-GlcNAc that defines the Golgi *N*-glycan-branching pathway in non-transformed epithelial cells (Lau et al. 2007). Briefly, multistep ultrasensitivity is due to declining affinities of Mgat1, Mgat2, Mgat4 and Mgat5 enzymes for UDP-GlcNAc (Km values increases from 0.04 to 10 mM across the pathway). Mgat1 overexpression has been shown to reduce substrate available to Mgat4 and Mgat5, but rescue is possible by extracellular GlcNAc supplementation to increase UDP-GlcNAc pool (Lau et al. 2007). Overexpression of Mgat4 and Mgat5 in malignant cells reduces pathway dependence on UDP-GlcNAc, thereby loss of regulator control by HBP (Lau and Dennis 2008).

Tet-induced Mgat5 HEK293 cells displayed a ~2-fold increase in tri-antennary (structure 3 and 5), and a ~2-fold increase in tetra-antennary (structure 8 and 11) *N*-glycans (Figure 3E). Tet-induced Mgat6 HEK293 cells produced the same novel oligosaccharide features observed in HeLa cells, predicted to be the 2,2,4,6 tetra- (structures 7 and 10), 4,2,2,4 tetra- (structures 9 and 12) and 4,2,2,4,6 penta- (structure 13), while native 4,2,2,6 tetra- (structures 8 and 11) were reduced (Figure 3F). The *N*-glycan profiling data for Mgat1, 5 and 6 Flp-In-TREx HeLa and HEK293 cells is summarized in Supplementary data, Figure S1.

Regulation of cellular metabolite levels by Mgat1, Mgat5, Mgat6 and HBP

Next, we measured metabolites in HeLa and HEK293 Flp-In-TREx cells by liquid chromatography–tandem mass spectrometry (LC–MS/MS) using MRM, targeting primarily glycolysis, amino acids, nucleotides, TCA cycle and HBP metabolites. Supplementing cells with GlcNAc increases UDP-GlcNAc available to the *N*-glycan-branching enzymes and should interact with tet-induced Mgat1, Mgat5 or Mgat6 to reveal more intense phenotypes (Sasai et al. 2002; Lau et al. 2007). Cells were cultured in standard nutrient-rich medium, with and without tet, in the presence of 0, 15 or 30 mM GlcNAc for 24 h, and cellular metabolites were extracted and analyzed by LC–MS/MS. In both Flp-In-TREx HeLa and HEK293 cells, GlcNAc supplementation increased intracellular UDP-GlcNAc up to ~5-fold over control. All metabolites quantified in this and other experiments are found in Supplementary data, Tables SI–III. Unsupervised clustering of metabolite data revealed that GlcNAc and tet-induced Mgat1,

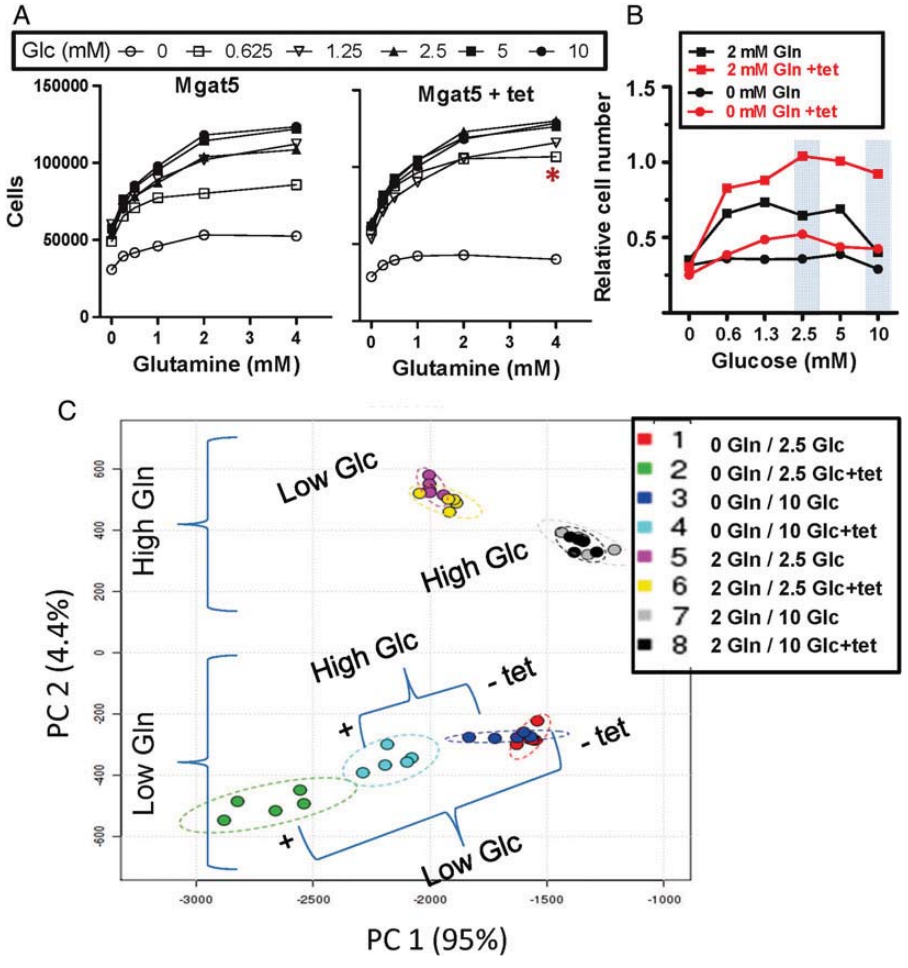

Fig. 5. Growth of Mgat5 Flp-In-TREx HEK293 cells in defined Glc and Gln conditions. Mgat5 Flp-In-TREx HEK293 clone 4 cells were cultured with and without tet in medium modified for Glc/Gln content as indicated + 10% FCS for 48 h. (**A**) Cell growth as a function of Glc and Gln concentrations, with and without tet-induced Mgat5 (cell count ± SD, $n = 3$). (**B**) Growth conditions (gray bars) corresponding to (**C**) metabolite profiling by LC–MS/MS, and analyzed by PCA (Supplementary data, Table SIV).

Mgat5 or Mgat6 increased the levels of many metabolites in HeLa cells, and HEK293 cells (Figure 4A). In the absence of GlcNAc, tet-induced Mgat1, Mgat5 or Mgat6 was associated with modest increases in metabolite levels, which was further enhanced in a dose-dependent manner by GlcNAc supplementation. For example, tet-induced Mgat5 and Mgat6 were additive with GlcNAc supplementation for increases in lactate in HEK293, suggesting increased glycolytic flux (Figure 4B; Supplementary data, Tables SII and SIII). Increased lactate production is commonly observed in proliferating cells, along with high rates of oxidative respiration that require mechanisms of stress tolerance (Levine and Puzio-Kuter 2010; Kaplon et al. 2013). Reactive oxygen species are toxic by-products

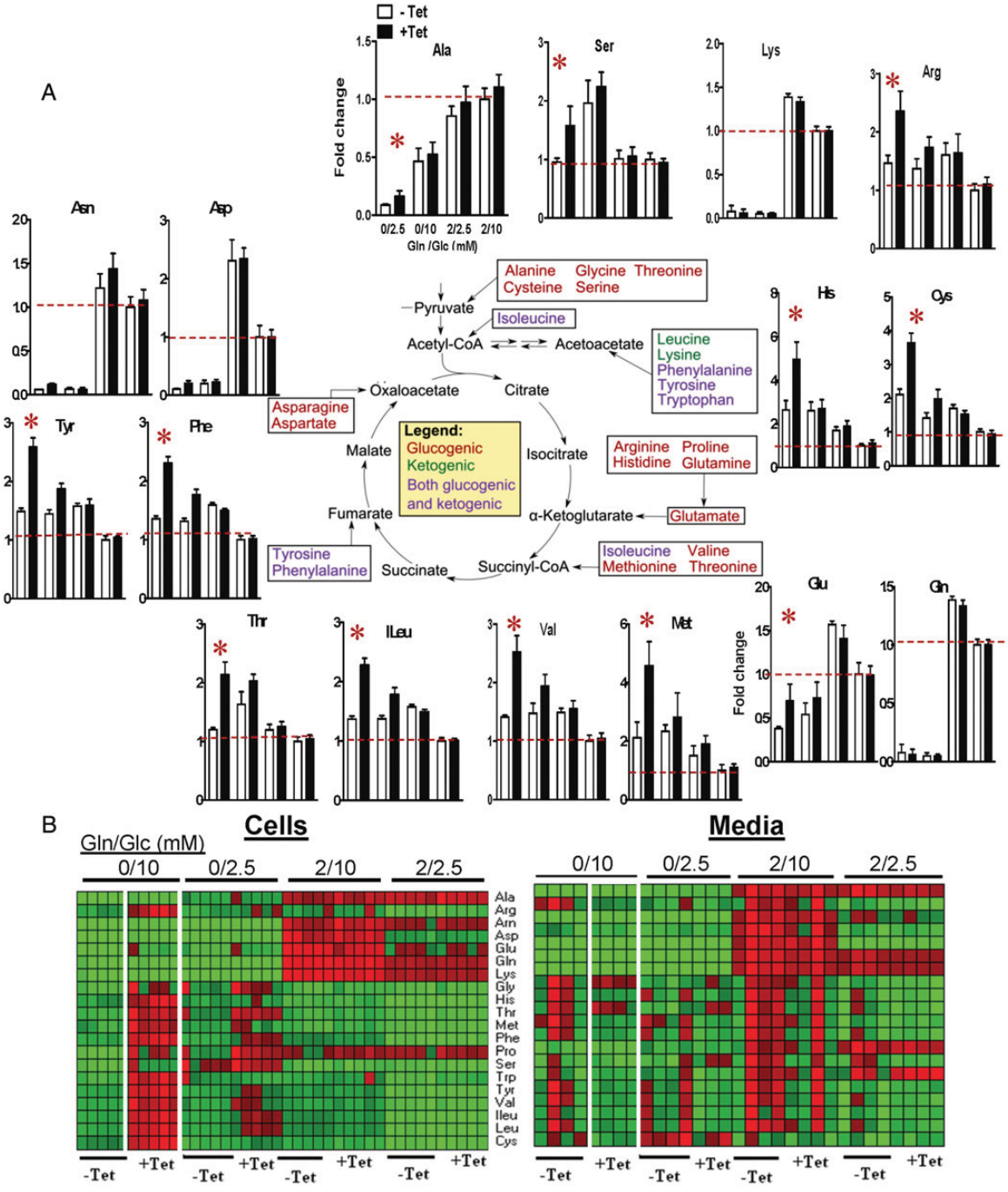

Fig. 6. Amino acid levels increase with Mgat5 expression in Gln-deprived conditions. (**A**) Mgat5 Flp-In-TREx HEK293 clone 4 cells were cultured in the four Gln/Glc conditions indicated, and data were normalized to 2.5/10 Gln/Glc no-tet (second bar from the right, red line) and plotted as fold change (mean ± SD, $n = 5$, $^*P < 0.05$). The axis labels are shown for Ala at the top. The pathway scheme is from Chapter 20 (Amino Acid Degradation and Synthesis) Lippincott's Illustrated Reviews: Biochemistry. (**B**) Heat map of amino acid levels in cells and medium showing data for each of 4–5 replicates. In limiting conditions, tet-induced Mgat5 increased cellular amino acids content, and the depleted growth medium of the same, indicating increased amino acids uptake. Red is high, green is low. White boxed area highlights contrasting effect of +tet on cells and medium.

of oxidative respiration that require buffering by glutathione (GSH) in a reaction that produces glutathione disulfide (GSSG) (Suzuki et al. 2010). The ratio of GSH to GSSG declined markedly with GlcNAc supplementation in HEK293 cells, with and without tet-induction for all three enzymes (Figure 4C). Mgat6 HEK293 cells displayed lower GSH/GSSG ratio without induction, which declined further with tet-induction and GlcNAc treatment, possibly due to low-level expression of Mgat6 in the absence of tet. Taken together, the results suggest that *N*-glycan branching and HBP increase the levels of many metabolites, including glycolysis and TCA cycle intermediates, as well as amino acids, with increased disposition of carbon into oxidative respiration (Figure 4D; Supplementary data, Tables SII and SIII). However, tet-induction and/or GlcNAc supplementation did not increase cell proliferation in the rich-medium conditions used in these experiments (Abdel Rahman et al. 2013; and data not shown).

Tet-inducible Mgat5 enhances amino acid uptake and growth in nutrient-poor conditions

Nutrient-rich culture medium does not reflect typical in vivo conditions, where Glc and amino acid availability are frequently limiting. Therefore, Glc and Gln were titrated in the medium, and cell growth compared for non-induced and tet-induced *N*-glycan branching. HeLa tumor cells displayed growth autonomy that did not benefit from tet-induced Mgat5 when Glc and/or Gln supply was limiting (data not shown). In contrast, tet-induced expression of Mgat5 alone in HEK293 cells rescued cell growth under low Glc/Gln conditions (Figure 5A). This is also consistent with the greater inducibility of Mgat5-branched *N*-glycans in the HEK293 cell line (Figures 2D and 3D). Therefore, HEK293 cells were cultured for 24 h in DMEM medium containing four Gln/Glc concentrations (0/2.5, 0/10, 2/2.5 and 2/10 mM), selected to reveal growth-sensitive effect of tet-induced Mgat5 (Figure 5A and B). Cellular metabolites were analyzed by LC–MS/MS, and principal component analysis (PCA) of the data revealed clear separation of the experimental groups based on Glc and Gln supply (Figure 5C). In 2 mM Gln, separation was observed for high versus low Glc, but no further separation was observed with tet-induced Mgat5, suggesting that Glc uptake is not likely the primary effect of tet-induced Mgat5. However, in 0 mM Gln, the tet-treated and untreated cells were separated, and with greater distance when Glc supply was also low (Figure 5C). Note that in 0 mM Gln without tet, Glc had no effect on separation in the PCA plot. We conclude that in Gln-depleted conditions, tet-induced Mgat5 enhances intracellular metabolite levels and growth by increasing amino acid uptake, while Glc supply acts as a modifying factor.

In Gln-depleted conditions, most metabolites that were measured increased with tet-induced Mgat5, while the effect of tet-induced Mgat5 in richer medium (i.e., 2 mM Gln plus 2.5 or 10 mM Glc)

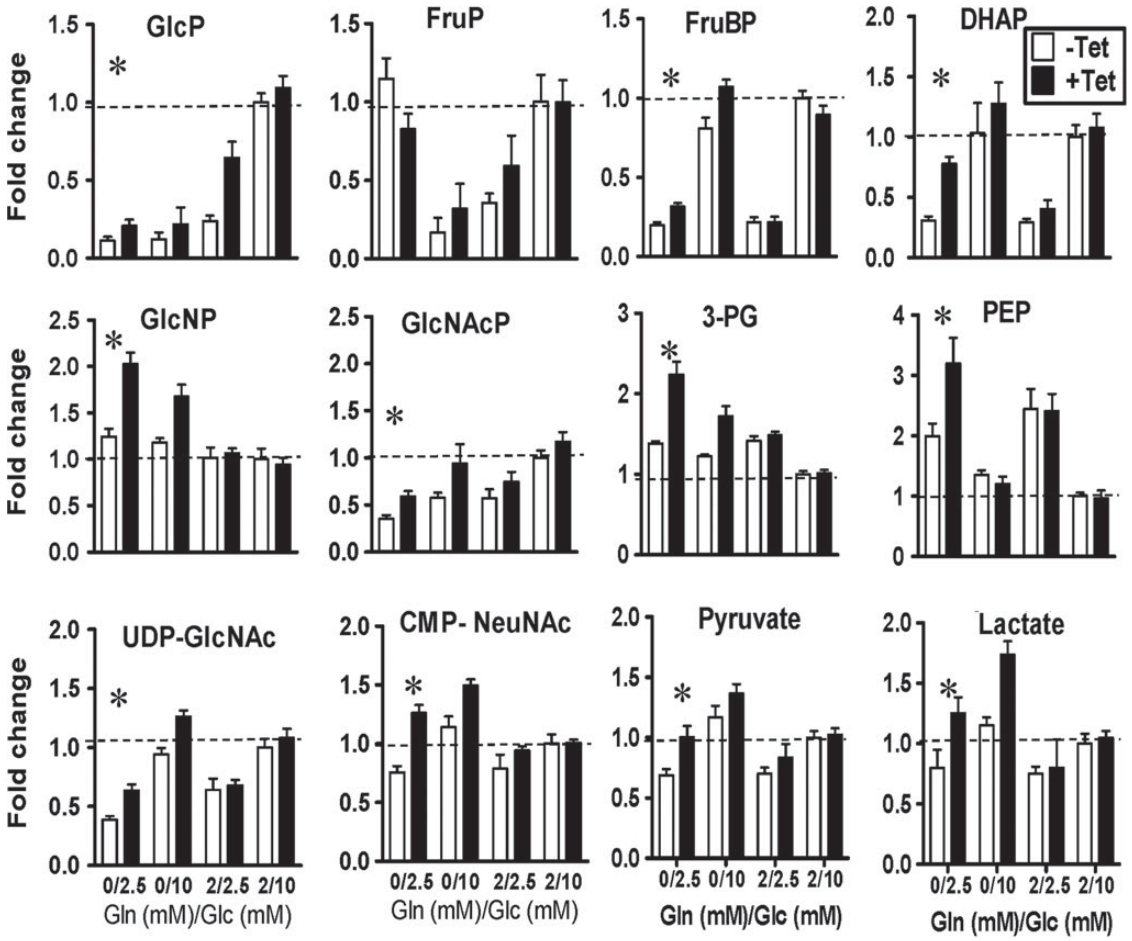

Fig. 7. Tet-induced Mgat5 increased HBP and glycolysis metabolites in Gln/Glc limiting conditions. Mgat5 Flp-In-TREx HEK293 clone 4 cells were cultured in the four Gln/Glc conditions, and normalized data graphed as fold change. The data were normalized to 2.5/10 mM Gln/Glc no-tet conditions (second bar from the right, black line). *$P < 0.05$ by Student's *t*-test for tet-induced change at 0/2.5 mM Gln/Glc condition.

was minimal (Figures 6 and 7). In Gln-depleted medium, intracellular Gln was reduced by ~10-fold, and Glu and α-ketoglutarate by ~2- to 3-fold (Figure 6A; Supplementary data, Figure S4). Tet-induced Mgat5 increased intracellular amino acid content, while depleting them from the growth media (Figure 6B). Increased consumption from the media by tet-induced Mgat5 cells was observed for Arg, His, Met, Phe, Ser, Trp, Tyr, Val, Ileu, Leu and Cys, which includes the essential amino acids (EAAs). The catabolism of amino acids provides NH_4^+ for Glu and Gln synthesis, as well as anaplerotic support to the TCA cycle. Indeed, tet-induced Mgat5 increased Glu and TCA cycle intermediates including succinyl-CoA, succinate, fumarate and malate (Supplementary data, Figure S4). Glycolysis and HBP intermediates were also increased in low Gln conditions, suggesting a reduced demand for Glc due to the increased uptake and catabolism of amino acids (Figure 7). Tet-induced Mgat5 increased GlcN-P, GlcNAc-P and UDP-GlcNAc, which contribute positive feedback to the *N*-glycan branching enzymes, and downstream effectors. Mgat5 has a low affinity for UDP-GlcNAc, and is therefore sensitive to Glc and Gln flux through HBP (Abdel Rahman et al. 2013). Our results suggest that up-regulation of Mgat5 may generate positive feedback to nutrient uptake by increasing UDP-GlcNAc supply to the Golgi (Figure 4D). The effect of tet-induced Mgat5 on central metabolite levels are summarized in Supplementary data, Figure S5.

Increased Gln uptake and catabolism is a critical feature of metabolism in proliferating cells (Levine and Puzio-Kuter 2010; Wellen and Thompson 2012). Branched-chain EAA uptake is mediated by a bidirectional transporter complex (Slc7a5 and Slc3a2) that exports Gln in exchange for the import of branched-chain EAA (Nicklin et al. 2009). To measure Gln uptake directly, cells were pulse labeled with dual-labeled $^{15}N^{15}N$-Gln for 1, 5 and 10 min. Tet-induced Mgat5 increased L-PHA staining by ~50% and modestly increased uptake of $^{15}N^{15}N$-Gln, which was further increased in an additive manner by 15 mM GlcNAc (Figure 8A). $^{15}N^{15}N$-Gln conversion to ^{15}N-Glu and re-amination to single-labeled ^{15}N-Gln showed similar kinetics (Figure 8, right). Tet-induced Mgat1 suppressed L-PHA staining by ~20%, consistent with observed suppression of tetra-antennary structures 8 and 11 by mass spectrometry (Figure 3D). Tet-induced Mgat1 alone had little effect on $^{15}N^{15}N$-Gln uptake (Figure 8B). These results demonstrate that Mgat5-modified *N*-glycan branching and HBP cooperate to up-regulate Gln import.

Discussion

In this report, we generated transgenic HEK293 and HeLa cell lines with single-site insertions for tet-inducible overexpression of Mgat1, Mgat5 and avian Mgat6 enzymes, and characterized their effects on *N*-glycan profiles and central metabolism by mass spectrometry. *N*-Glycan profiling revealed unexpected differences between HeLa and HEK293 cell lines following tet-inducible transgene overexpression. In HeLa cells, tet-induced Mgat1 markedly increased the expected hybrid *N*-glycans, but had a much smaller effect on downstream branching, suggesting the cells have insufficient α-mannosidase

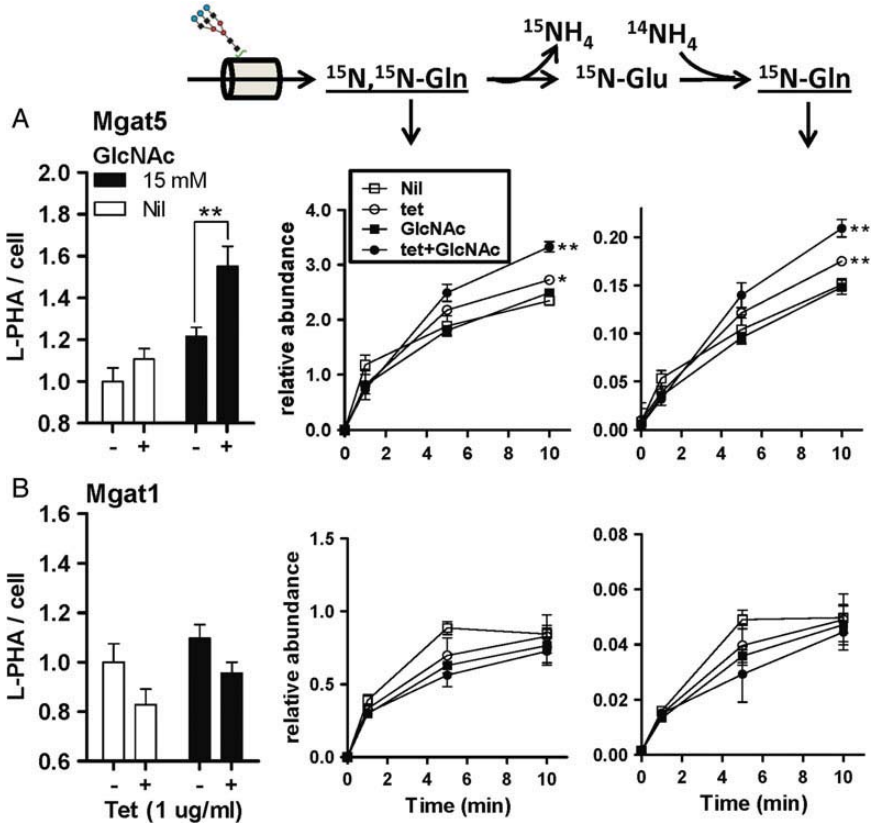

Fig. 8. Tet-induced Mgat5 branching stimulates Gln uptake. Flp-In-TREx HEK293 (**A**) Mgat5 clone 4 and (**B**) Mgat1 clone 7 cells were grown with and without tet and 15 mM GlcNAc in standard culture conditions. Gln was removed for 16 h and cells were pulsed with 1 mM $^{15}N^{15}N$ Gln for the indicated times. $^{15}N^{15}N$ Gln and ^{15}N Gln levels in cell lysates were measured by LC–MS/MS. $*P < 0.05$ and $**P < 0.01$ with $n = 5$–6 samples. The bar graphs on the left compare branching by L-PHA staining of Mgat1 and Mgat5, with and without tet-induction.

II activity to process the additional Mgat1 product. In HEK293 cells, tet-induced Mgat1 did not increase hybrid *N*-glycans, but did partially suppress downstream branching, consistent with previous characterization of the pathway as multistep ultrasensitive to UDP-GlcNAc (Lau et al. 2007, 2008). Tet-induced Mgat5 increased tri- and tetra-antennary *N*-glycans in HEK293 more robustly than in HeLa cells. HBP supplementation was additive with tet-induced Mgat1, Mgat5 and Mgat6 for increasing levels of cellular metabolites in nutrient-rich medium. The nutrients were not a stimulus for cell proliferation, but rather catabolism as indicated by increased lactate and oxidative respiration. GlcNAc supplementation at >15 mM overcame the UDP-GlcNAc-limiting effects of Mgat1 overexpression in HEK293T cells (Lau et al. 2007). Similarly, GlcNAc supplementation acts downstream of α-mannosidase II and Mgat1, and markedly up-regulated metabolite levels in HeLa cells.

Mgat6 enhances functionality of *N*-glycan branching in mammalian cells

The Mgat5 product is the preferred acceptor for Mgat6, which adds a GlcNAcβ1,4 branch that is not present in mammals (Watanabe et al. 2006). The mature *N*-glycan branches function in an additive manner to regulate galectin binding to growth factor receptors and nutrient transporters at the cell surface (Lau et al. 2007). Here, we have tested the hypothesis from an evolutionary perspective. The addition of an ectopic branch to *N*-glycans in mammalian cells should display an additive and stronger phenotypic effect compared with overexpression of Mgat5. Tet-induced Mgat6 alone and with GlcNAc supplementation in both HeLa and HEK293 cell lines, displayed the strongest enhancement of metabolite levels of the three enzymes tested (Figure 4A). It is possible that overexpression of Mgat6 qualitatively changes the interaction between mammalian branching enzymes and HBP, or that Mgat6 has substrate preferences that alter the relationship between nutrient transporters activities. Overall, our results provide compelling evidence that functional redundancy of branches and their conditional regulation by HBP is a critical feature of metabolic regulation (Dennis and Brewer 2013). The emergence of Mgat6 in tetrapod dinosaurs and retention of the gene in modern birds may play a critical role in their metabolic rates and fitness.

Mgat5 enhances metabolism in Gln-deprived conditions

In low Gln/Glc culture conditions, tet-induced Mgat5 alone rescued proliferation in cultures of HEK293 cells, but not in HeLa cells, consistent with the relative change in *N*-glycan branching upon tet-Mgat5 induction in the two cell lines. Tet-induced Mgat5 in HEK293 cells stimulated the uptake of EAAs, and increased the levels of glycolytic, HBP and TCA pathway intermediates (Figures 6 and 7). In a more direct assay of uptake, tet-induced Mgat5 and 15 mM GlcNAc-stimulated $^{15}N^{15}N$-Gln uptake in a cooperative manner (Figure 8). GlcNAc supplementation to HBP has been shown to stimulate Gln uptake and catabolism in $Bax^{-/-}Bak^{-/-}$ lymphoma cells in the absence of Glc (Wellen et al. 2010). In these experiments, surface IL-3 receptor was reduced in Glc-starved condition, but could be rescued by GlcNAc supplementation to UDP-GlcNAc and *N*-glycan branching (Wellen et al. 2010). Furthermore, IL-3 receptor-dependent signaling-stimulated transcription of SLC1A5, a high-affinity Gln transporter, and SLC6A19, a transporter of Leu and Gln. However, the present study is the first to show a direct effect of Mgat5-mediated branching on amino acid uptake and metabolic flux, in low Gln/Glc (i.e., 0/2.5 mM) +10% FBS culture conditions. Gln is not an EAA, but high growth rates in embryonic and cancer cells depend on the import of Gln, and anaplerotic conversion to α-ketoglutarate which supports the TCA cycle (DeBerardinis et al. 2008). SLC7A5/SLC3A2 is a bidirectional transporter that imports branched-chain essential amino acids (BCAAs) (Leu, Ile and Val) in exchange for Gln efflux (Nicklin et al. 2009). The Gln transporter, SLC1A5 is widely expressed and required to support BCAA uptake, although in some cells, Gln biosynthesis from α-ketoglutarate and glutamate can support internal needs and SLC7A5/SLC3A2 activity (Hassanein et al. 2013). Tet-induced Mgat5 alone in HEK293 cells was sufficient to increase uptake of Gln and EAA in low Gln/Glc culture conditions. Gln is also a positive regulator of HBP (Abdel Rahman et al. 2013) and may drive reciprocal positive feedback between *N*-glycan branching and metabolism (Figure 4D; Supplementary data, Figure S5).

Mgat5-deficient mice are hypoglycemic and display a reduced sensitivity to glucagon (Johswich et al. 2014), and here we have presented the first evidence of cell autonomous regulation of metabolism by *N*-glycan branching. Up-regulation of Mgat5 in HEK293 cells stimulated amino acid uptake and increased metabolite levels under low Gln/Glc culture conditions. Further work is required to identify the various nutrient transporters regulated by *N*-glycan branching and their contribution to development, disease and environmental stress.

Supplementary data

Supplementary data for this article are available online at http://glycob.oxfordjournals.org/.

Acknowledgements

The authors thank Aldis Krizus, Amy Woroch and Kevin Yau for excellent technical assistance, and Dr Stephen Taylor (University of Manchester) for the kind gift of Flp-In-TREx HeLa cells.

Conflict of interest statement

None declared.

Funding

Research described in this manuscript was supported by grants from Canadian Cancer Society (2010-7000444), MRI-ORF GL2, CIHR (MOP-62975) and The Sydney C. Cooper Program for the Prevention of Cancer Progression to J.W.D. A.A.R. was supported by MITACS-Accelerate, and M.R. was supported by the Frank Fletcher Memorial Fund, Mary Gertrude I'Anson Scholarship and Paul Starita Graduate Student Fellowship. Metabolomics data have been deposited at ftp://PASS00385:PU9246h@ftp.peptideatlas.org/.

Abbreviations

BCAAs, branched-chain essential amino acids; ConA, concanavalin A; EAAs, essential amino acids; ESI, electrospray ionization; FBS, fetal bovine serum; Glc, glucose; GlcNAc, acetylglucosamine; Gln, glutamine; Gluts, Glc transporters; GSH, glutathione; GSSG, glutathione disulfide; HBP, hexosamine biosynthesis pathway; L-PHA, leucoagglutinin; MRM, multiple reaction monitoring; PBS, phosphate-buffered saline; PCA, principal component analysis; tet, tetracycline

References

Abdel Rahman AM, Ryczko M, Pawling J, Dennis JW. 2013. Probing the hexosamine biosynthetic pathway in human tumor cells by multitargeted tandem mass spectrometry. *ACS Chem Biol*. 8:2053–2062.

Abdel Rahman AM, Pawling J, Ryczko M, Dennis JW. 2014. Targeted metabolomics in cultured cells and tissues by mass spectrometry: Method development and validation. *Anal Chim Acta*. 845:53–61.

Beheshti Zavareh R, Sukhai MA, Hurren R, Gronda M, Wang X, Simpson CD, Maclean N, Zih F, Ketela T, Swallow CJ, et al. 2012. Suppression of cancer progression by MGAT1 shRNA knockdown. *PLoS ONE*. 7:e43721.

Buckhaults P, Chen L, Fregien N, Pierce M. 1997. Transcriptional regulation of N-acetylglucosaminyltransferase V by the src Oncogene. *J Biol Chem*. 272:19575–19581.

Cheung P, Dennis JW. 2007. Mgat5 and Pten interact to regulate cell growth and polarity. *Glycobiology*. 17:767–773.

Cheung P, Pawling J, Partridge EA, Sukhu B, Grynpas M, Dennis JW. 2007. Metabolic homeostasis and tissue renewal are dependent on beta1,6GlcNAc-branched N-glycans. *Glycobiology*. 17:828–837.

D'Arrigo A, Belluco C, Ambrosi A, Digito M, Esposito G, Bertola A, Fabris M, Nofrate V, Mammano E, Leon A, et al. 2005. Metastatic transcriptional pattern revealed by gene expression profiling in primary colorectal carcinoma. *Int J Cancer*. 115:256–262.

DeBerardinis RJ, Lum JJ, Hatzivassiliou G, Thompson CB. 2008. The biology of cancer: Metabolic reprogramming fuels cell growth and proliferation. *Cell Metab*. 7:11–20.

Demetriou M, Nabi IR, Coppolino M, Dedhar S, Dennis JW. 1995. Reduced contact-inhibition and substratum adhesion in epithelial cells expressing GlcNAc-transferase V. *J Cell Biol*. 130:383–392.

Dennis JW, Brewer CF. 2013. Density-dependent lectin-glycan interactions as a paradigm for conditional regulation by posttranslational modifications. *Mol Cell Proteomics*. 12:913–920.

Dennis JW, Kosh K, Bryce D-M, Breitman ML. 1989. Oncogenes conferring metastatic potential induce increased branching of Asn-linked oligosaccharides in rat2 fibroblasts. *Oncogene*. 4:853–860.

Fernandes B, Sagman U, Auger M, Demetriou M, Dennis JW. 1991. Beta1–6 branched oligosaccharides as a marker of tumor progression in human breast and colon neoplasia. *Cancer Res*. 51:718–723.

Frauwirth KA, Riley JL, Harris MH, Parry RV, Rathmell JC, Plas DR, Elstrom RL, June CH, Thompson CB. 2002. The CD28 signaling pathway regulates glucose metabolism. *Immunity*. 16:769–777.

Granovsky M, Fata J, Pawling J, Muller WJ, Khokha R, Dennis JW. 2000. Suppression of tumor growth and metastasis in Mgat5-deficient mice. *Nature Med*. 6:306–312.

Haga Y, Ishii K, Suzuki T. 2011. N-Glycosylation is critical for the stability and intracellular trafficking of glucose transporter GLUT4. *J Biol Chem*. 286:31320–31327.

Hassanein M, Hoeksema MD, Shiota M, Qian J, Harris BK, Chen H, Clark JE, Alborn WE, Eisenberg R, Massion PP. 2013. SLC1A5 mediates glutamine transport required for lung cancer cell growth and survival. *Clin Cancer Res*. 19:560–570.

Johswich A, Longuet C, Pawling J, Rahman AA, Ryczko M, Drucker DJ, Dennis JW. 2014. N-Glycan remodeling on glucagon receptor is an effector of nutrient sensing by the hexosamine biosynthesis pathway. *J Biol Chem*. 289:15927–15941.

Kang R, Saito H, Ihara Y, Miyoshi E, Koyama N, Sheng Y, Taniguchi N. 1996. Transcriptional regulation of the N-acetylglucosaminyltranserase V gene in human bile duct carcinoma cells (HuCC-T1) is mediated by Ets-1. *J Biol Chem*. 271:26706–26712.

Kaplon J, Zheng L, Meissl K, Chaneton B, Selivanov VA, Mackay G, van der Burg SH, Verdegaal EM, Cascante M, Shlomi T, et al. 2013. A key role for mitochondrial gatekeeper pyruvate dehydrogenase in oncogene-induced senescence. *Nature*. 498:109–112.

Kitagawa T, Tsuruhara Y, Hayashi M, Endo T, Stanbridge EJ. 1995. A tumor-associated glycosylation change in the glucose transporter GLUT1 controlled by tumor suppressor function in human cell hybrids. *J Cell Sci*. 108:3735–3743.

Korczak B, Le T, Elowe S, Donavan R, Datti A, Dennis JW. 2000. Minimal Catalytic Domain of N-Acetylglucosaminyltransferase V. *Glycobiology*. 10:595–599.

Lau K, Partridge EA, Silvescu CI, Grigorian A, Pawling J, Reinhold VN, Demetriou M, Dennis JW. 2007. Complex N-glycan number and degree of branching cooperate to regulate cell proliferation and differentiation. *Cell*. 129:123–134.

Lau KS, Dennis JW. 2008. N-Glycans in cancer progression. *Glycobiology*. 18:750–760.

Lau KS, Khan S, Dennis JW. 2008. Genome-scale identification of UDP-GlcNAc-dependent pathways. *Proteomics*. 8:3294–3302.

Levine AJ, Puzio-Kuter AM. 2010. The control of the metabolic switch in cancers by oncogenes and tumor suppressor genes. *Science*. 330:1340–1344.

Nakano M, Saldanha R, Gobel A, Kavallaris M, Packer NH. 2011. Identification of glycan structure alterations on cell membrane proteins in desoxyepothilone B resistant leukemia cells. *Mol Cell Proteomics*. 10:M111 009001.

Nicklin P, Bergman P, Zhang B, Triantafellow E, Wang H, Nyfeler B, Yang H, Hild M, Kung C, Wilson C, et al. 2009. Bidirectional transport of amino acids regulates mTOR and autophagy. *Cell*. 136:521–534.

Ohtsubo K, Takamatsu S, Minowa MT, Yoshida A, Takeuchi M, Marth JD. 2005. Dietary and genetic control of glucose transporter 2 glycosylation promotes insulin secretion in suppressing diabetes. *Cell*. 123:1307–1321.

Partridge EA, Le Roy C, Di Guglielmo GM, Pawling J, Cheung P, Granovsky M, Nabi IR, Wrana JL, Dennis JW. 2004. Regulation of cytokine receptors by Golgi N-glycan processing and endocytosis. *Science*. 306:120–124.

Sasai K, Ikeda Y, Fujii T, Tsuda T, Taniguchi N. 2002. UDP-GlcNAc concentration is an important factor in the biosynthesis of beta1,6-branched oligosaccharides: Regulation based on the kinetic properties of N-acetylglucosaminyltransferase V. *Glycobiology*. 12:119–127.

Schachter H. 1986. Biosynthetic controls that determine the branching and microheterogeneity of protein-bound oligosaccharides. *Biochem Cell Biol*. 64:163–181.

Seelentag WK, Li WP, Schmitz SF, Metzger U, Aeberhard P, Heitz PU, Roth J. 1998. Prognostic value of beta1,6-branched oligosaccharides in human colorectal carcinoma. *Cancer Res*. 58:5559–5564.

Shirato K, Nakajima K, Korekane H, Takamatsu S, Gao C, Angata T, Ohtsubo K, Taniguchi N. 2011. Hypoxic regulation of glycosylation via the N-acetylglucosamine cycle. *J Clin Biochem Nutr*. 48:20–25.

Soliman MA, Abdel Rahman AM, Lamming DA, Birsoy K, Pawling J, Frigolet ME, Lu H, Fantus IG, Pasculescu A, Zheng Y, et al. 2014. The adaptor protein p66Shc inhibits mTOR-dependent anabolic metabolism. *Sci Signal*. 7:ra17.

Song Y, Aglipay JA, Bernstein JD, Goswami S, Stanley P. 2010. The bisecting GlcNAc on N-glycans inhibits growth factor signaling and retards mammary tumor progression. *Cancer Res*. 70:3361–3371.

Suzuki S, Tanaka T, Poyurovsky MV, Nagano H, Mayama T, Ohkubo S, Lokshin M, Hosokawa H, Nakayama T, Suzuki Y, et al. 2010. Phosphate-activated glutaminase (GLS2), a p53-inducible regulator of glutamine metabolism and reactive oxygen species. *Proc Natl Acad Sci USA*. 107:7461–7466.

Taguchi T, Ogawa T, Inoue S, Inoue Y, Sakamoto Y, Korekane H, Taniguchi N. 2000. Purification and characterization of UDP-GlcNAc: GlcNAcbeta 1–6 (GlcNAcbeta 1–2)Manalpha 1-R [GlcNAc to Man]-beta 1, 4-N-acetylglucosaminyltransferase VI from hen oviduct. *J Biol Chem*. 275:32598–32602.

Takamatsu S, Antonopoulos A, Ohtsubo K, Ditto D, Chiba Y, Le DT, Morris HR, Haslam SM, Dell A, Marth JD, et al. 2010. Physiological and glycomic characterization of N-acetylglucosaminyltransferase-IVa and -IVb double deficient mice. *Glycobiology*. 20:485–497.

Takamatsu S, Oguri S, Minowa MT, Yoshida A, Nakamura K, Takeuchi M, Kobata A. 1999. Unusually high expression of N-acetylglucosaminyltransferase-IV a in human choriocarcinoma cell lines: A possible enzymatic basis of the formaiton of abnormal biantennary sugar chain. *Cancer Res*. 59:3949–3953.

Varki A, Cummings RD, Esko J, Freeze H, Stanley P, Bertozzi C, Hart GW, Etzler ME. 2009. *Essentials of Glycobiology*. New York: Cold Spring Harbor Laboratory.

Ward RJ, Alvarez-Curto E, Milligan G. 2011. Using the Flp-In T-Rex system to regulate GPCR expression. *Methods Mol Biol*. 746:21–37.

Watanabe T, Ihara H, Miyoshi E, Honke K, Taniguchi N, Taguchi T. 2006. A specific detection of GlcNAcbeta1–6Manalpha1 branches in N-linked glycoproteins based on the specificity of N-acetylglucosaminyltransferase VI. *Glycobiology*. 16:431–439.

Wellen KE, Lu C, Mancuso A, Lemons JM, Ryczko M, Dennis JW, Rabinowitz JD, Coller HA, Thompson CB. 2010. The hexosamine

biosynthetic pathway couples growth factor-induced glutamine uptake to glucose metabolism. *Genes Dev*. 24:2784–2799.

Wellen KE, Thompson CB. 2012. A two-way street: Reciprocal regulation of metabolism and signalling. *Nat Rev Mol Cell Biol*. 13:270–276.

Wise DR, DeBerardinis RJ, Mancuso A, Sayed N, Zhang XY, Pfeiffer HK, Nissim I, Daikhin E, Yudkoff M, McMahon SB, et al. 2008. Myc regulates a transcriptional program that stimulates mitochondrial glutaminolysis and leads to glutamine addiction. *Proc Natl Acad Sci USA*. 105:18782–18787.

Xia J, Mandal R, Sinelnikov IV, Broadhurst D, Wishart DS. 2012. MetaboAnalyst 2.0--a comprehensive server for metabolomic data analysis. *Nucleic Acids Res*. 40:W127–W133.

Ying H, Kimmelman AC, Lyssiotis CA, Hua S, Chu GC, Fletcher-Sananikone E, Locasale JW, Son J, Zhang H, Coloff JL, et al. 2012. Oncogenic Kras maintains pancreatic tumors through regulation of anabolic glucose metabolism. *Cell*. 149:656–670.

Yoshimura M, Nishikawa A, Ihara Y, Taniguchi S, Taniguchi N. 1995. Suppression of lung metastasis of B16 mouse melanoma by N-acetylglucosaminyltransferase III gene transfection. *Proc Natl Acad Sci USA*. 92:8753–8758.

Yun J, Rago C, Cheong I, Pagliarini R, Angenendt P, Rajagopalan H, Schmidt K, Willson JK, Markowitz S, Zhou S, et al. 2009. Glucose deprivation contributes to the development of KRAS pathway mutations in tumor cells. *Science*. 325:1555–1559.